

This copy is for your personal, non-commercial use only.

If you wish to distribute this article to others, you can order high-quality copies for your colleagues, clients, or customers by [clicking here](#).

Permission to republish or repurpose articles or portions of articles can be obtained by following the guidelines [here](#).

The following resources related to this article are available online at www.sciencemag.org (this information is current as of July 13, 2010):

Updated information and services, including high-resolution figures, can be found in the online version of this article at:

<http://www.sciencemag.org/cgi/content/full/326/5954/818>

Supporting Online Material can be found at:

<http://www.sciencemag.org/cgi/content/full/326/5954/818/DC1>

A list of selected additional articles on the Science Web sites **related to this article** can be found at:

<http://www.sciencemag.org/cgi/content/full/326/5954/818#related-content>

This article **cites 26 articles**, 13 of which can be accessed for free:

<http://www.sciencemag.org/cgi/content/full/326/5954/818#otherarticles>

This article has been **cited by** 37 article(s) on the ISI Web of Science.

This article has been **cited by** 13 articles hosted by HighWire Press; see:

<http://www.sciencemag.org/cgi/content/full/326/5954/818#otherarticles>

This article appears in the following **subject collections**:

Medicine, Diseases

<http://www.sciencemag.org/cgi/collection/medicine>

Hematopoietic Stem Cell Gene Therapy with a Lentiviral Vector in X-Linked Adrenoleukodystrophy

Nathalie Cartier,^{1,2*} Salima Hacein-Bey-Abina,^{3,4,5*} Cynthia C. Bartholomae,⁶ Gabor Veres,⁷ Manfred Schmidt,⁶ Ina Kutschera,⁶ Michel Vidaud,¹ Ulrich Abel,⁶ Liliane Dal-Cortivo,^{3,5} Laure Caccavelli,^{3,5} Nizar Mahlaoui,⁸ Véronique Kiermer,⁹ Denice Mittelstaedt,¹⁰ Céline Bellesme,² Najiba Lahlou,¹¹ François Lefrère,³ Stéphane Blanche,⁸ Muriel Audit,¹² Emmanuel Payen,^{13,14} Philippe Leboulch,^{13,14,15} Bruno l'Homme,¹ Pierre Bougnères,² Christof Von Kalle,⁶ Alain Fischer,^{4,8} Marina Cavazzana-Calvo,^{3,4,5*} Patrick Aubourg^{1,2*†}

X-linked adrenoleukodystrophy (ALD) is a severe brain demyelinating disease in boys that is caused by a deficiency in ALD protein, an adenosine triphosphate-binding cassette transporter encoded by the *ABCD1* gene. ALD progression can be halted by allogeneic hematopoietic cell transplantation (HCT). We initiated a gene therapy trial in two ALD patients for whom there were no matched donors. Autologous CD34⁺ cells were removed from the patients, genetically corrected ex vivo with a lentiviral vector encoding wild-type *ABCD1*, and then re-infused into the patients after they had received myeloablative treatment. Over a span of 24 to 30 months of follow-up, we detected polyclonal reconstitution, with 9 to 14% of granulocytes, monocytes, and T and B lymphocytes expressing the ALD protein. These results strongly suggest that hematopoietic stem cells were transduced in the patients. Beginning 14 to 16 months after infusion of the genetically corrected cells, progressive cerebral demyelination in the two patients stopped, a clinical outcome comparable to that achieved by allogeneic HCT. Thus, lentiviral-mediated gene therapy of hematopoietic stem cells can provide clinical benefits in ALD.

X-linked adrenoleukodystrophy [(ALD), Online Mendelian Inheritance in Man database number 300100] is a fatal demyelinating disease of the central nervous system (CNS) caused by mutations of the *ABCD1* gene encoding the ALD protein, an adenosine triphosphate-binding cassette transporter localized in the membrane of peroxisomes. The ALD protein participates in the peroxisomal degrada-

tion of very-long-chain fatty acids (VLCFAs) in oligodendrocytes and microglia, and deficiency of this protein disrupts myelin maintenance by these cells (1). Affected boys enter a phase of active multifocal brain demyelination when they are 6 to 8 years old. Most die before reaching adolescence. Allogeneic hematopoietic cell transplantation (HCT) is the only effective therapy to date, provided that it can be performed at an early stage of brain lesions (2, 3). Beyond a certain stage, demyelination cannot be arrested. The long-term benefits of HCT in ALD are mediated by the replacement of brain microglial cells derived from donor bone marrow myelo-monocytic cells (4, 5). Because the potential of HCT is limited by donor-related constraints and carries a considerable risk of mortality, we reasoned that hematopoietic stem cell (HSC) gene therapy could be an appropriate therapeutic alternative.

Lentiviral vectors, such as those derived from HIV-1, can transduce nondividing cells and allow (both in vitro and in mice) a more efficient gene transfer into HSCs than murine gamma-retrovirus (γ RV) vectors (6, 7). For diseases like ALD, we did not expect that the limitations of γ RV in HSC transduction could be overcome, because the genetically corrected hematopoietic cells have no growth advantage over unmodified cells. However, the greater efficiency of lentiviral vectors in HSC transduction suggested that gene correction might be achieved in a high percentage of HSCs and would therefore result in long-term expression of the

therapeutic gene in all hematopoietic cell lineages of treated patients (8).

ALD gene transfer with lentiviral vectors in vitro has yielded biochemical correction of monocytes/macrophages derived from ALD protein-deficient human CD34⁺ cells (9). In vivo, the transplantation of lentivirally transduced murine ALD Sca-1⁺ cells (a functional equivalent of CD34⁺ cells in humans) into ALD mice resulted in the replacement of 20 to 25% of brain microglial cells expressing the ALD protein 12 months after transplantation (10) (fig. S1). Unfortunately, because the ALD mouse does not develop cerebral demyelination (11), the neuropathological and clinical effects of lentiviral gene transfer could not be assessed in this model. When lentivirally transduced human ALD CD34⁺ cells were transplanted into nonobese diabetic/severe combined immunodeficient (NOD/SCID) mice, the recipient mice showed in vivo expression of ALD protein in human monocytes and macrophages derived from engrafted human stem cells (9). More importantly, human bone marrow-derived cells were shown to migrate into the brain of recipient mice and then differentiate into microglia expressing the human ALD protein (12).

Ex vivo lentiviral-mediated transfer of the *ABCD1* gene into CD34⁺ cells from ALD patients. On the basis of these promising preclinical data and our past experience in treating more than 35 ALD patients by HCT, we initiated a study of lentiviral-mediated HSC gene therapy in two ALD patients who had progressive cerebral demyelination and adrenal insufficiency and who had no human leukocyte antigen (HLA)-matched donor or cord blood for allogeneic HCT. These two patients, aged 7.5 years (P1) and 7 years (P2), had *ABCD1* gene mutations (a large deletion from exon 6 in P1 and E609K mutation in P2), resulting in the absence of ALD protein detectable by immunocytochemistry in fibroblasts and white blood cells. Peripheral blood mononuclear cells (PBMCs) were taken from the patients after stimulation by intravenous injection of granulocyte colony-stimulating factor. After positive selection by an immunomagnetic procedure, CD34⁺ cells were pre-activated ex vivo with a mixture of cytokines (10). The cells were then infected with a replication-defective HIV-1-derived lentiviral vector (CG1711 hALD) expressing wild-type *ABCD1* cDNA under the control of the MND (myeloproliferative sarcoma virus enhancer, negative control region deleted, dl587rev primer binding site substituted) promoter (10). Transduced CD34⁺ cells were frozen so that we could perform replication-competent lentivirus assays (10) before re-infusion. Cryopreserved transduced CD34⁺ cells (4.6×10^6 and 7.2×10^6 cells per kilogram, respectively) were thawed and infused into P1 and P2, after a fully myeloablative conditioning regimen with cyclophosphamide and busulfan. Because lentiviral correction does not provide human or mouse ALD HSCs with a

¹INSERM UMR745, University Paris-Descartes, 75279 Paris, France. ²Department of Pediatric Endocrinology and Neurology, Hôpital Saint-Vincent de Paul, Assistance Publique-Hôpitaux de Paris, 82 Avenue Denfert-Rochereau, 75674 Paris, France. ³Department of Biotherapy, Hôpital Necker-Enfants Malades, 75743 Paris, France. ⁴INSERM UMR768, University Paris-Descartes, 75743 Paris, France. ⁵Clinical Investigation Center in Biotherapy, Groupe Hospitalier Universitaire Ouest, Assistance Publique-Hôpitaux de Paris (Inserm), 75743 Paris, France. ⁶National Center for Tumor Diseases and German Cancer Research Center (Deutsches Krebsforschungszentrum), 69120 Heidelberg, Germany. ⁷117 Southwest 72nd Place, Gainesville, FL 32608, USA. ⁸Department of Pediatric Immunohematology, Hôpital Necker-Enfants Malades, 75743 Paris, France. ⁹Nature Publishing Group, New York, NY 10013-1917, USA. ¹⁰13687 Quinton Road, San Diego, CA 92129, USA. ¹¹Department of Biochemistry, Hôpital Saint-Vincent de Paul, 75674 Paris, France. ¹²Genosafe, 91002 Evry, France. ¹³Commissariat à l'Énergie Atomique (CEA), Institute of Emerging Diseases and Innovative Therapies (iMETI), Fontenay-aux-Roses 92265, France. ¹⁴INSERM U962 and Université de Paris XI, CEA-iMETI, Fontenay-aux-Roses 92265, France. ¹⁵Genetics Division, Brigham and Women's Hospital and Harvard Medical School, Boston, MA 02115, USA.

*These authors contributed equally to this work.

†To whom correspondence should be addressed. E-mail: patrick.aubourg@inserm.fr

selective growth advantage, we used a full myeloablation regimen, as this step would most likely increase the engraftment of transduced HSCs by removal of resident non-transduced HSCs. We observed that 50% (P1) and 33% (P2) of infused CD34⁺ cells expressed the ALD protein, as shown by immunofluorescence (10) 5 days after transduction. The lentivirally encoded ALD protein showed enzymatic activity, resulting in 55% (P1) to 68% (P2) reduction of VLCFA levels in transduced CD34⁺ cells (10). The mean number of integrated provirus copies per cultured CD34⁺ cell was 0.7 and 0.6 for P1 and P2, respectively, 5 days after transduction (10). The procedure was clinically uneventful. Hematopoietic recovery occurred at days 13 to 15 after transplant and was sustained thereafter.

Expression of lentivirally encoded ALD protein in patient's hematopoietic cells after autologous transplantation of gene-corrected CD34⁺ cells. At day +30 after infusion, ALD protein was expressed in 23 and 25% of peripheral blood mononuclear cells from P1 and

P2, respectively (Fig. 1A). In P1, the percentage of PBMCs expressing lentivirally encoded ALD protein decreased to 13% at 9 months after transplant and has stabilized to ~10% at 30 months after transplant (Fig. 1A). In P2, ALD protein expression decreased to 17% at 9 months after transplant and has stabilized to 15% at 24 months after transplant (Fig. 1A). ALD protein expression correlated well with the mean number of integrated vector copies in the same cells (P1, 0.14 copies per cell, 30 months after transplant; P2, 0.20 copies per cell, 24 months after transplant) (10). VLCFA levels were reduced by 20 and 28% in the PBMCs from P1 and P2 at 24 and 20 months posttransplant, respectively.

In both patients, the lentivirally encoded ALD protein was expressed at percentages between 9 and 14% in the different CD14⁺, CD19⁺, CD3⁺, and CD15⁺ peripheral blood lineages, in samples taken 24 to 30 months after transplantation (Fig. 1, B and C). Expression of ALD protein in bone marrow CD34⁺ cells (purity > 99%) went from 20 and 18% (12 months) to 18% (24 months) and

17% (20 months) in P1 and P2, respectively. Similarly, vector-derived sequences were present in 17.3% of colony-forming units–granulocyte-macrophage (CFU-GM) in P1, 24 months after HSC gene therapy, indicating effective gene transfer into common myeloid progenitors with long-term engraftment capacity.

Longitudinal analysis of lentiviral vector insertion and clonal hematopoiesis after autologous transplantation of gene-corrected CD34⁺ cells. The clonal distribution of gene-modified cells in vivo was studied prospectively by a large-scale analysis of lentivirus insertion sites (ISs) with high-throughput 454 pyrosequencing of linear amplification–mediated polymerase chain reaction (LAM-PCR) amplicon (13). Clonal contributions to patient cells were visualized as different size bands representing the multitude of ISs (Fig. 2, A and B). The sensitivity of LAM-PCR combined with next generation sequencing permits the determination of entire insertion repertoires and thereby allows the physiology and kinetics of hematopoietic repopulation to be studied in detail. For LAM-PCR, we applied a combination of restriction enzymes according to an algorithm that allows the amplification of sequences covering all known genomic sequences. LAM-PCR on >98% enriched CD14⁺, CD15⁺, CD3⁺, C19⁺, and bone marrow CD34⁺ cells revealed a high number of distinct ISs, indicating a consistently polyclonal distribution of lentivirally corrected hematopoietic cells over time (Fig. 2, A and B). A total of 2217 (P1) and 1380 (P2) unique LAM-PCR amplicons obtained from patient cell samples before (P1, 501; P2, 484) and after transplantation (P1, 1719; P2, 900) were unequivocally mapped to specific positions in the human genome (14). Collision between samples may arise from the combination of exquisitely sensitive LAM-PCR with deep-sequencing technologies, creating false-positive sequence reads. Collision reads were excluded with the use of a predefined algorithm (10). Typical for lentiviral integrants, insertions were distributed mainly in gene coding regions (P1, 72.71%; P2, 75.80%), without a particular preference for transcriptional start sites, and frequently occurred in chromosomes harboring gene-dense regions (fig. S2) (15).

To determine whether HSCs had been transduced, we compared ISs of lentiviral vector in purified lymphoid CD3⁺ and CD19⁺ cells and myeloid CD14⁺ and CD15⁺ cells from P1 and P2 after transplant, as well as in their CFU-GM colonies derived from posttransplant bone marrow CD34⁺ cells. 86 out of 1846 ISs (myeloid, 940 ISs; lymphoid, 906 ISs) in P1 (4.6%) and 12 ISs out of 835 ISs (myeloid, 578 ISs; lymphoid, 247 ISs) in P2 (1.4%) occurred in both lymphoid and myeloid cells (Fig. 2, C and D). To estimate whether sharing ISs between different lineages could be indicative of initially transduced primitive hematopoietic progenitor cells, we calculated *P* values under the null hypothesis that insertions would follow a Poisson

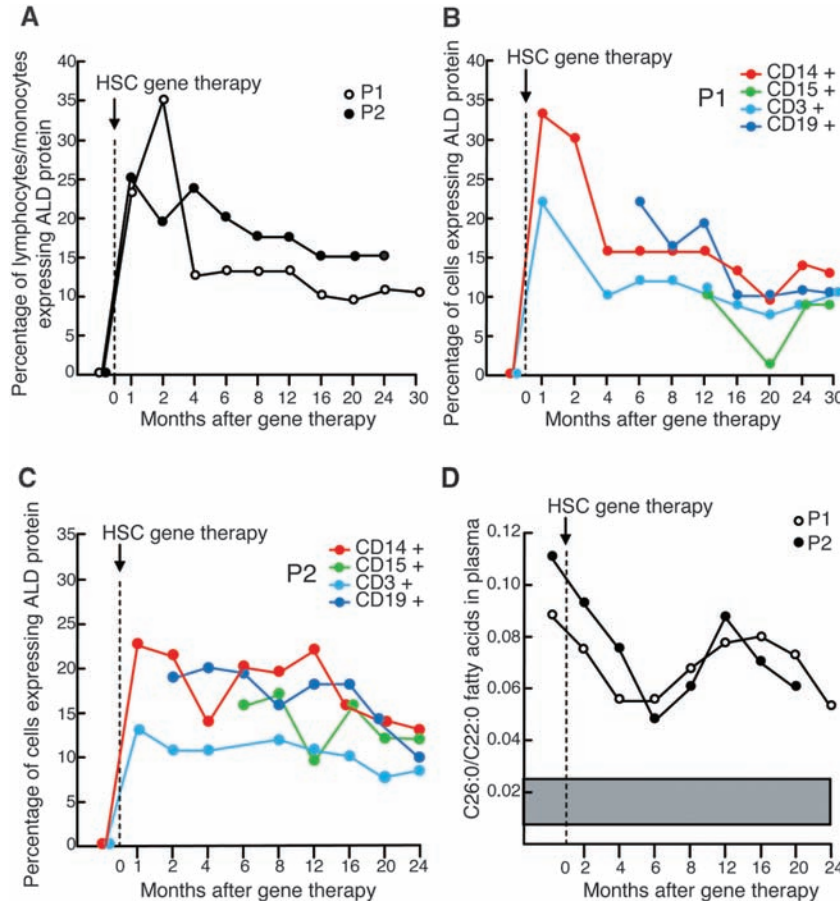


Fig. 1. Gene marking in P1 and P2 after HSC gene therapy. (A) Percentage of peripheral blood lymphocytes and monocytes expressing ALD protein before and after HSC gene therapy. Lymphocytes and monocytes were isolated on a Ficoll gradient and analyzed for the expression of ALD protein after immunostaining with an anti-ALD protein monoclonal antibody (mAb) (12). (B and C) Expression of ALD protein in monocytes (CD14⁺), granulocytes (CD15⁺), T lymphocytes (CD3⁺), and B lymphocytes (CD19⁺) from P1 and P2. Cells were purified on microbeads with appropriate mAbs, and purity (>99%) was checked on a FACS cell sorter. Cells were then analyzed for the expression of ALD protein using an anti-human ALD protein mAb (16). (D) Plasma levels of VLCFAs expressed as C26:0/C22:0 ratio in P1 and P2 before and after HSC gene therapy. The gray band indicates the normal mean \pm SD of C26:0/C22:0 fatty acid ratio.

distribution with expected value E (10). The observed numbers of identities [86 (P1) and 12 (P2), respectively] were at least 22,000 (P1) and 18,000 times (P2) higher than the values expected by chance alone; i.e., they were calculated on the basis of a uniform random IS distribution both over the coding and the non-coding regions ($P = 0$). We used quantitative reverse transcription polymerase chain reaction (RT-PCR) to verify that cross-contamination of CD3⁺ cells and CD14⁺ cells was below 0.2 to 0.4%. Even if one assumes a hypothetical 2% contamination rate by fluorescence-activated cell sorting (FACS), the observed identities in both lineages were still at least 16,000 times higher than the expected values (10). These data indicate that a substantial number of clones with lymphoid and myeloid lineage capability exist and that lentiviral transduction of HSCs had been achieved.

To monitor for early signs of vector-induced dominance of individual clones, we determined the quantitative contribution of individual clones to gene-corrected hematopoiesis by ordering all distinct ISs according to their abundance in every deep-sequencing run on samples containing more than 300 ng of DNA. (Fig. 3, A and B). The retrieval frequency (sequence count) of identical ISs in insertion repertoires obtained by high-throughput sequencing allows a good estimate of clonal contribution, provided that the analyses are performed in samples with comparable clonality, contain a sufficient amount of DNA (13), and an optimized choice of restriction enzymes avoids bias in the amplification of ISs by LAM-PCR. Clonal distribution varied, and no frequent clone re-appeared with an increasing count. No dominance emerged among active hematopoietic clones in the two patients. We also monitored whether the distribution of RefSeq genes with vector insertions changed over time. Insertions affecting the same gene or genomic region in two or more individual cell clones, termed common integration sites (CISs), can indicate that insertion in this particular locus might enhance clonal engraftment, survival or proliferation. No significant difference existed after sample-size adjustment in the proportion of CIS in cells sampled after re-infusion (P1, 30.71%; P2, 15.74%) compared with those sampled before re-infusion [P1, 8.58%; P2, 9.30%] (fig. S3).

We analyzed the gene classes targeted by the lentiviral vector using ingenuity pathway analysis. We found individual gene classes enriched in engrafted cells, but these classes differed between P1 and P2 (fig. S4). Although certain CIS or changes in gene-class enrichment might be related to vector insertion, these findings are currently without known biological or clinical relevance and will be monitored in the molecular follow-up of our patients.

Neuroradiological and neurologic outcomes in ALD patients treated by HSC gene therapy. Before HSC gene therapy, the magnetic resonance imaging (MRI) scan of P1 showed an

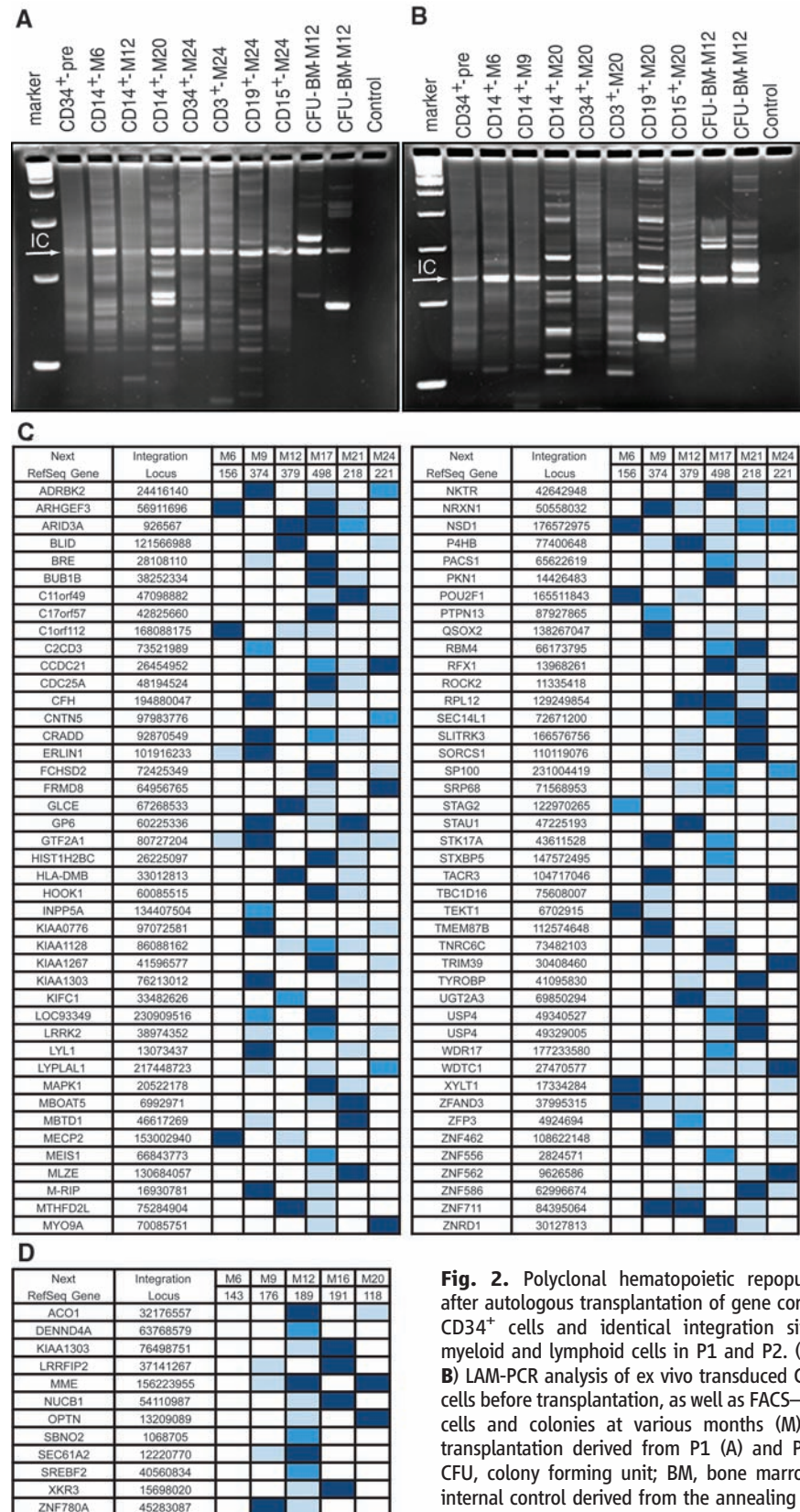


Fig. 2. Polyclonal hematopoietic repopulation after autologous transplantation of gene corrected CD34⁺ cells and identical integration sites in myeloid and lymphoid cells in P1 and P2. (A and B) LAM-PCR analysis of ex vivo transduced CD34⁺ cells before transplantation, as well as FACS-sorted cells and colonies at various months (M) after transplantation derived from P1 (A) and P2 (B). CFU, colony forming unit; BM, bone marrow; IC, internal control derived from the annealing of the LAM-PCR primers to the 5'LTR sequences. (C and D)

Identical insertion sites found in myeloid (CD14⁺, CD15⁺, CFU-GM) and lymphoid (CD3⁺, CD19⁺) sorted cells in P1 (C) and P2 (D). Light blue, IS identified in myeloid cells at the same timepoint; medium blue, IS identified in myeloid and lymphoid cells at the same timepoint; dark blue, IS identified in lymphoid cells at the same timepoint. See table S1 for a detailed overview of identical IS found in the different sorted cell fractions over time.

abnormal hyperintensity signal that reflected demyelination of pyramidal tracts within the brain stem, pons, internal capsulae, and the periventricular frontal white matter, scored at 2.25 (maximum score = 34 points) (16) (Fig. 4A). Enhanced gadolinium contrast indicated that the demyelinating lesions were inflammatory and disrupted the blood-brain barrier (fig. S5). Contrast enhancement of demyelinating lesions disappeared completely 12 months after transplant (fig. S5). Demyelinating lesions continued to extend into the frontal white matter up to month 14 (demyelination score of 6.75), but since then have remained unchanged (Fig. 4A). Before HSC gene therapy, P2 had more extensive demyelinating lesions (Fig. 4B) than P1, with abnormal hyperintensity signal in the splenium of the corpus callosum, the white matter of parieto-occipital lobes, and the auditory pathways scored at 7 (Fig. 4B). Gadolinium contrast enhancement disappeared 9 months after transplant. A minimal contrast enhancement had reappeared in P2 16 months after transplant at the anterior edge of the left parietal white matter lesions, but it has not been detected since then (fig. S5). Lesions extended into the posterior parietal white matter up to 16 months after gene therapy but have remained stable since then (Fig. 4B). The hyperintensity signal involving the auditory pathways disappeared completely, indicating reversal of demyelination, a process that does not occur spontaneously in ALD. Thus, the demyelinating score of P2 remained at 7, as it was before gene

therapy, despite the extension of lesions in the parietal white matter. These results are in sharp contrast with the continuous progression of cerebral demyelination in untreated ALD patients (Fig. 4C), but they are similar to what is typically observed after allogeneic HCT (2, 3). During the first 12 to 24 months after HCT, a brain MRI usually shows a progression of the demyelinating lesions, aggravating the demyelination score by 5 to 6 points out of 34 (3). The demyelinating lesions then stabilize or even reverse, as observed here, with no further changes for decades (2, 3).

The neurologic outcomes of P1 and P2 were also reminiscent of successful allogeneic HCT (3). In untreated ALD patients, the decline of performance and verbal functions is inevitably continuous and devastating during the first 2 years after the onset of inflammatory demyelinating lesions (1). In 40% of ALD patients treated by allogeneic HCT, an initial decline of performance abilities without changes in verbal abilities is followed by stabilization (3). Before HSC gene therapy, P1 had normal neurologic examination and normal verbal intelligence (quotient of 108) but moderate nonverbal performance disability (quotient of 99). After gene therapy, his verbal intelligence has remained unchanged (quotient of 104). An initial decline in nonverbal performance (quotient of 74) has stabilized. He developed muscle weakness on the right side of the body at month 7, which then started to improve until nearly complete regres-

sion by month 14 after transplant. The motor and cognitive functions of P2 were normal before and remained so after HSC gene therapy (verbal and performance of 103 and 111, respectively, 20 months after gene therapy), with the exception of a persistent defect in the lower quadrants of the visual field that appeared 14 months after transplant and has remained stable thereafter. The myeloablative conditioning regimen is unlikely to have contributed to these clinical benefits. Of four patients showing a failure or a marked delay to engraft after this conditioning regimen in our allotransplantation series, all uniformly developed devastating progression of cerebral demyelination and cognitive decline.

Plasma VLCFA levels of ALD patients decrease by ~55% after allogeneic HCT (3), mostly reflecting replacement of liver macrophages by donor-derived cells. Plasma VLCFA levels were reduced by 39% in P1 and 38% in P2, 24 and 20 months after the transplant, respectively (Fig. 1D). Considering that liver macrophages and peripheral blood monocytes originate from the same myeloid precursors, this correction of plasma VLCFA was greater than expected, given that only 13 to 14% of peripheral blood monocytes expressed the ALD transgene in P1 and P2. Similar overcorrection of VLCFA accumulation was observed in PBMCs and transduced CD34⁺ cells from P1 and P2, possibly reflecting ALD protein overexpression or a preferential engraftment of corrected extravascular monocytes/macrophage progenitors early after infusion.

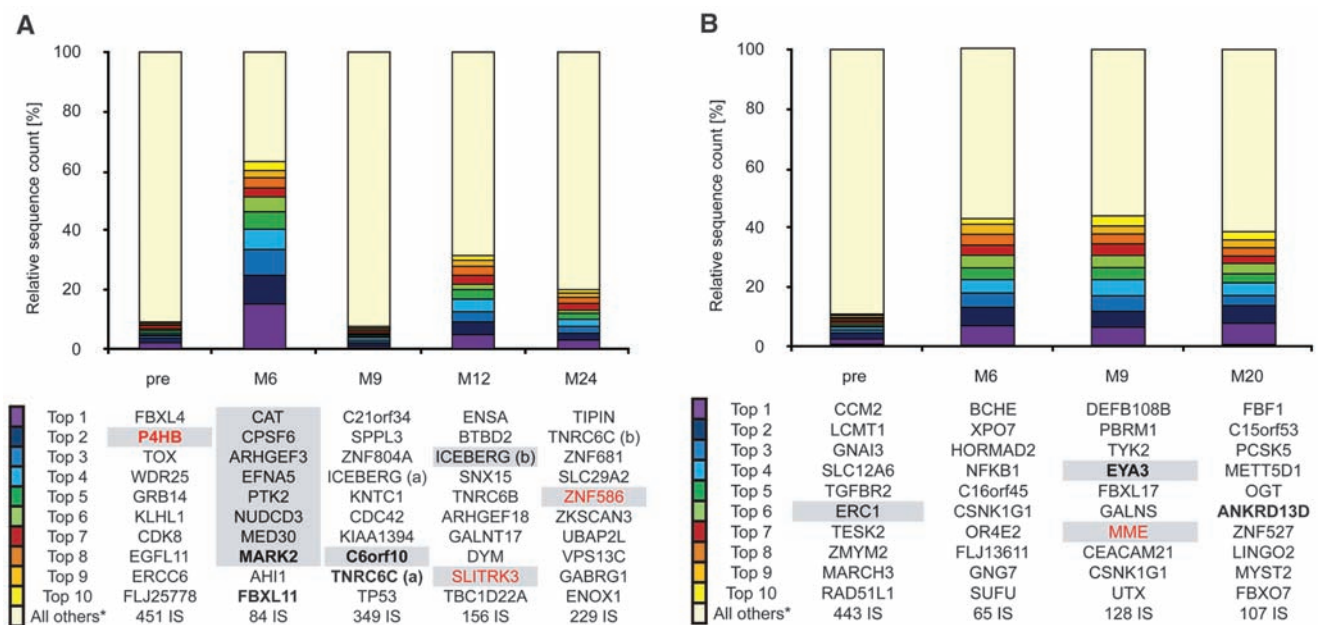


Fig. 3. Retrieval frequency (relative sequence count) of individual integration sites in sequenced polyclonal cell samples from P1 (A) and P2 (B). The quantitative clonal contribution of individually gene corrected cells was assessed by counting identical integration site sequences after 454 pyrosequencing of LAM-PCR amplicons. The relative contribution of individual amplicons is given as the percentage of all insertion flank sequence reads encountered in the particular sample. The 10 most frequent ISs are ranked from 1 to 10, according to frequency. None of the most frequent ISs re-appeared or were found to

contribute a large or growing portion of gene-modified cells to the circulation over extended periods of time. There was no obvious limitation to the clonal repertoire nor was there a clonal dominance. Genes listed in boldface were associated with multiple ISs in different clones (CISs), those listed in red were associated with ISs in both the lymphoid and the myeloid lineages, and those genes highlighted in gray were associated with ISs at more than one timepoint. All others*, all less frequently encountered genetic locations that harbor ISs in the respective sample analyzed.

Quantitative RT-PCR of PBMCs from P1 and P2 showed that the *ABCD1* transgene was expressed at a four- to fivefold higher level than the endogenous mutated *ABCD1* gene (table S2) (10).

Discussion. Previous genetic correction of human HSCs with a murine γ RV vector was successful only in the setting of immunodeficiency disorders such as adenosine deaminase deficiency and severe combined immunodeficiency–X1 (SCID-X1), in which the transgene conferred a selective growth advantage to lymphocytes derived from transduced HSCs (17–20). Lentiviral vectors based on HIV-1 are potentially superior to γ RV vectors, particularly in short-term transduction protocols that minimize ex vivo cell manipulation, because they can be used to transduce candidate HSCs from patients and because they maintain sustained transgene expression even when the genetically corrected HSCs do not acquire a growth advantage (21, 22). In the present trial, the long-term stability of ALD pro-

tein expression in myeloid cells, as well as the presence over time of identical ISs in both the myeloid and lymphoid lineages, strongly suggest that HSCs have been transduced with the capacity to self-renew and repopulate multiple hematopoietic lineages.

The adverse events that occurred in SCID-X1 patients treated with γ RV vector gene therapy have raised serious concerns about retroviral integration-related mutagenesis and leukemogenesis (23). Transcriptionally active long terminal repeats (LTRs) of retroviral vectors are major determinants of genotoxicity (24), whereas the LTR promoter/enhancer of lentiviral vector used in this study is self-inactivating (SIN) upon transduction. This and other differences in lentiviral and oncoretroviral biology suggest that the risk of insertional mutagenesis by a SIN lentiviral vector may be lower than that with γ RVs and even SIN γ RVs (24–26). In our study, we took advantage of new deep-sequencing technol-

ogies for genome-wide monitoring of lentivirus-marked HSC clonality in the patients. Although we did not detect obvious clonal skewing or dominance in hematopoiesis, a longer follow-up and a larger sample size will be required to verify that the potential for genotoxicity of lentiviral vectors in this application is low.

Before this gene therapy trial, we did not know how many corrected HSCs would need to be infused to achieve clinically relevant neurological benefit, because this crucial issue could not be addressed in the phenotypically normal ALD mouse (11). We only knew that all affected ALD boys who were successfully treated by allogeneic HCT and showed stabilization and/or regression of cerebral demyelination had more than 80% donor-derived engraftment (2, 3). In the current study, long-lasting expression of ALD protein in ~15% of monocytes (CD14⁺), a population of cells that have the same myelomonocytic origin as bone marrow-derived brain microglia (27), was sufficient to obtain comparable neurological benefits after gene transfer into autologous HSCs, probably because ALD protein is overexpressed in microglial cells that derive from transduced CD34⁺ cells (28). Further studies will be needed to test the balance between less toxic partial myeloablation and the need for effective engraftment of transduced HSCs.

The fact that the neurologic benefits of HSC gene therapy in ALD were comparable to those seen with allogeneic HCT supports further testing of this treatment in an extended series of ALD patients with cerebral demyelination who do not have an available HLA-matched donor or cord blood. HSC gene therapy might also be considered as a therapeutic option for adult ALD patients who develop cerebral demyelination, for whom the mortality risk of allogeneic HCT is ~40%. Finally, the recruitment of bone marrow-derived cells to CNS macrophages/microglia may provide a new avenue for cell-based gene therapy in other genetic and multifactorial CNS diseases.

References and Notes

1. H. W. Moser, A. Mahmood, G. V. Raymond, *Nat. Clin. Pract. Neurol.* **3**, 140 (2007).
2. P. Aubourg et al., *N. Engl. J. Med.* **322**, 1860 (1990).
3. E. Shapiro et al., *Lancet* **356**, 713 (2000).
4. M. A. Eglitis, E. Mezey, *Proc. Natl. Acad. Sci. U.S.A.* **94**, 4080 (1997).
5. J. Priller et al., *Nat. Med.* **7**, 1356 (2001).
6. L. Naldini et al., *Science* **272**, 263 (1996).
7. H. Miyoshi, K. A. Smith, D. E. Mosier, I. M. Verma, B. E. Torbett, *Science* **283**, 682 (1999).
8. M. A. Kay, J. C. Glorioso, L. Naldini, *Nat. Med.* **7**, 33 (2001).
9. S. Benhamida et al., *Mol. Ther.* **7**, 317 (2003).
10. Materials and methods and other supporting material are available on Science Online.
11. A. Pujol et al., *Hum. Mol. Genet.* **11**, 499 (2002).
12. M. Asheuer et al., *Proc. Natl. Acad. Sci. U.S.A.* **101**, 3557 (2004).
13. M. Schmidt et al., *Nat. Methods* **4**, 1051 (2007).
14. Data of 3597 unique LAM-PCR amplicons are available as open access database at <https://consort.gatc-biotech.com/lampcr/>. For username and password, please contact the corresponding author.

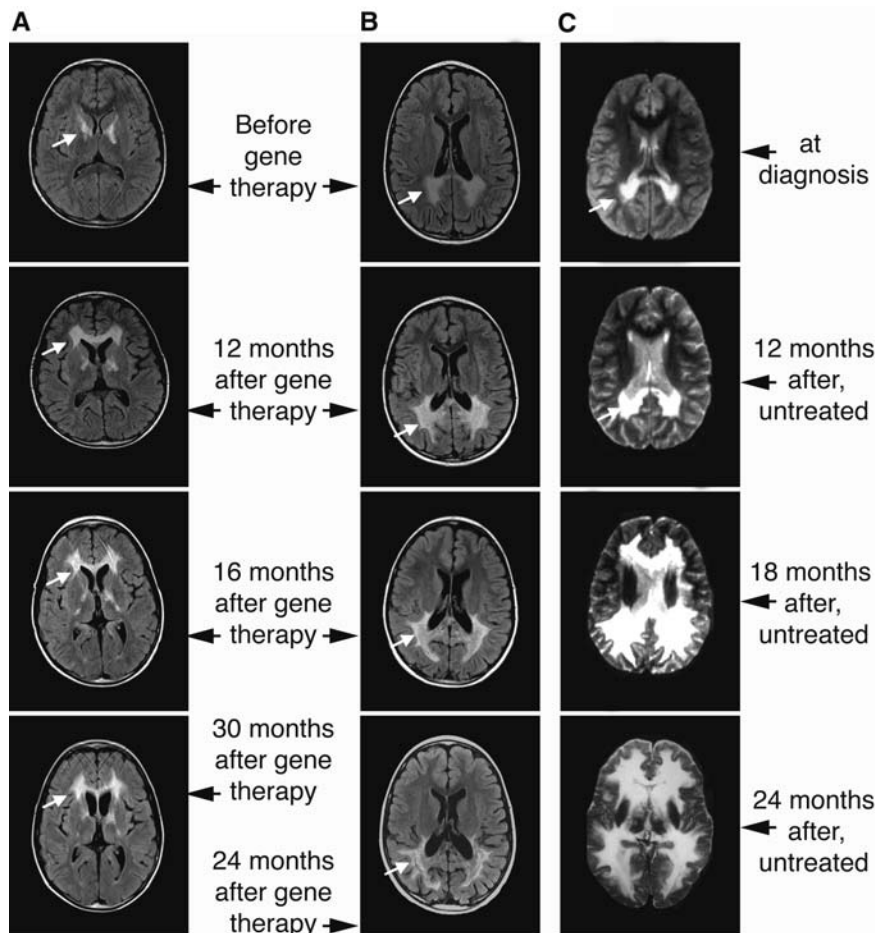


Fig. 4. Brain MRIs from P1 (A) and P2 (B) before and after gene therapy. (A) Fluid attenuated inversion recovery (FLAIR) sequences show hypersignal involving the pyramidal tracts within the internal capsule (white arrows) and periventricular frontal white matter of P1 before gene therapy. These lesions extended into the frontal white matter up to 14 months after HSC gene therapy and then did not show progression. (B) In P2, FLAIR sequences show hypersignal involving the corpus callosum, the parieto-occipital white matter (white arrows), and the auditory pathways before gene therapy. These lesions extended into the white matter of posterior parietal lobes up to 16 months after gene therapy and then stabilized with no further progression. (A and B) A mild dilation of frontal (P1) or occipital (P2) horns of ventricle is present 20 to 24 months after gene therapy. (C) Progression of cerebral demyelinating lesions in an untreated 8-year-old ALD patient (demyelination score at 26, 24 months after diagnosis).

15. A. R. W. Schröder *et al.*, *Cell* **110**, 521 (2002).
16. D. J. Loes *et al.*, *Am. J. Neuroradiol.* **15**, 1761 (1994).
17. M. Cavazzana-Calvo *et al.*, *Science* **288**, 669 (2000).
18. S. Hacein-Bey-Abina *et al.*, *N. Engl. J. Med.* **346**, 1185 (2002).
19. H. B. Gaspar *et al.*, *Lancet* **364**, 2181 (2004).
20. A. Aiuti *et al.*, *N. Engl. J. Med.* **360**, 447 (2009).
21. N. Uchida *et al.*, *Proc. Natl. Acad. Sci. U.S.A.* **95**, 11939 (1998).
22. W. Piacibello *et al.*, *Blood* **100**, 4391 (2002).
23. S. Hacein-Bey-Abina *et al.*, *Science* **302**, 415 (2003).
24. E. Montini *et al.*, *J. Clin. Invest.* **119**, 964 (2009).
25. M. De Palma *et al.*, *Blood* **105**, 2307 (2005).
26. E. Montini *et al.*, *Nat. Biotechnol.* **24**, 687 (2006).
27. N. Davoust, C. Vuallat, C. Androdias, S. Nataf, *Trends Immunol.* **29**, 227 (2008).
28. A. Biffi *et al.*, *J. Clin. Invest.* **116**, 3070 (2006).
29. We thank A. Salzman and R. Salzman for their continuous help and support in this project; the pediatricians and nurses of the Unité d'Endocrinologie et Neurologie Pédiatriques, Hôpital Saint-Vincent de Paul and the Unité d'Immunologie et d'Hématologie Pédiatriques, Hôpital Necker-Enfants Malades for patient care; A. Pujol

and C. Sever Bermejo for patient referral; C. Adamsbaum for neuroimaging studies; F. Audat for cytopheresis; P. Lebon for HIV and VSV.G serologies; C. Lagresle-Peyrou for setting up the transduction protocol; P. Working and Cell Genesys staff for the lenti-MND-ALD vector; PeproTech for SCF, Flt-3, MGDF, and IL-3 cytokines; Takara Bio for the CH-296 fibronectin fragment; and E. Postaire and C. Sebastiani at INSERM. P.A. and N.C. were supported by grants from INSERM, European Leukodystrophy Association, Association Française contre les Myopathies, La Fondation de France, the STOP-ALD foundation, La Fondation Avenir, Etablissement Français des Greffes, Thermo Fisher Scientific, the 6th Framework European Economic Community (EEC) Programme (LSHM-CT2004-502987) and the Programme Hospitalier de Recherche Clinique (AOM 3043, French Health Ministry). S.H.-B.-A., L.D.-C., L.C., F.L., A.F., and M.C.-C. were supported by INSERM, Assistance Publique-Hôpitaux de Paris, Centre d'Investigation Clinique-Biotherapy, and Association Française contre les Myopathies. C.V.K. and M.S. were supported by grants from the Deutsche

Forschungsgemeinschaft (SPP 1230), the German Ministry of Education and Research (TREATID), the Helmholtz Association, and the 6th Framework EEC Programme (CONCERT, CLINIGENE). P. Leboulch owns stock in Genetix Pharmaceuticals, and G. Veres, V. Kiermer, and D. Mittelstaedt were formerly employed at Cell Genesys. This gene therapy trial was approved by AFSSAPS on 15 November 2005 and CCPRB Paris-Cochin (local Institutional Review Board) on 7 September 2004. Informed consent was obtained from the parents of the patients after the nature and possible consequences of the studies were explained.

Supporting Online Material

www.sciencemag.org/cgi/content/full/326/5954/818/DC1
Materials and Methods
SOM Text
Figs. S1 to S5
Tables S1 and S2
References

22 January 2009; accepted 4 September 2009
10.1126/science.1171242

REPORTS

Three-Color Entanglement

A. S. Coelho,¹ F. A. S. Barbosa,¹ K. N. Cassemiro,² A. S. Villar,^{2,3} M. Martinelli,¹ P. Nussenzveig^{1*}

Entanglement is an essential quantum resource for the acceleration of information processing as well as for sophisticated quantum communication protocols. Quantum information networks are expected to convey information from one place to another by using entangled light beams. We demonstrated the generation of entanglement among three bright beams of light, all of different wavelengths (532.251, 1062.102, and 1066.915 nanometers). We also observed disentanglement for finite channel losses, the continuous variable counterpart to entanglement sudden death.

Since Schrödinger defined entanglement as “the characteristic trait of quantum mechanics” (1), much study has been devoted to its understanding. Possible applications to information tasks such as storage, computation, and communications have generated a large amount of research (2). Quantum computing is expected to be more efficient than its classical counterpart, and there are quantum algorithms (3) that greatly surpass the best classical ones. Quantum communications can, in principle, provide absolute security (4). Nevertheless, many technological challenges remain, because the quantum resources are fragile and undergo decoherence from their inevitable interactions with the surrounding environment (5). Furthermore, many fundamental issues regarding the nature and dynamics of entanglement remain to be understood (6).

A variety of physical systems are currently under investigation to perform the envisioned information tasks (7–12). Because each one has

its advantages and disadvantages, it is likely that several of them will be combined to perform reliable quantum information tasks. Light, in view of its high speed and weak interaction with the environment, is a strong candidate to convey quantum information by using quantum teleportation (13, 14). To connect such different physical systems (typically lacking a joint resonance) at the nodes of a quantum network (15), however, different frequencies of light will be necessary. For two such beams, entanglement has already been demonstrated, ranging from small frequency differences (16, 17) up to one frequency being twice the other (18). It is important to go beyond just two beams for multi-mode networks. Our demonstration used three field modes with different wavelengths.

Our system is an optical parametric oscillator (OPO), which consists of a nonlinear optical crystal inside a cavity, so that the fields are fed back into the system. Light that is incident on the crystal undergoes parametric down-conversion, a process whereby an incident photon is converted into a pair of longer-wavelength photons, fulfilling energy conservation $\omega_0 = \omega_1 + \omega_2$, where the ω_i ($i = 0, 1, 2$) values are the angular frequencies of the incident light and of the two generated photons, respectively. Momentum is also conserved, corresponding to the phase-

matching condition. Owing to the cavity feedback, down-converted photons can be emitted in occupied field modes, a process known as stimulated emission, with increasing probability as the number of photons in the mode grows, thus providing gain. When the pump laser power is increased, the gain overcomes the losses and the system oscillates. Above this oscillation threshold, tripartite entanglement has been predicted (19). Down-converted photons are produced in pairs, yielding strong intensity correlations among the twin beams. To produce twin photons, a pump photon must be annihilated; thus, anti-correlations are expected between the reflected pump intensity and the sum of twin beams' intensities. The frequency constraint translates into a constraint for the phase variations (or fluctuations) of the three fields. The twins' phase fluctuations should be anticorrelated, and their sum should be correlated to the pump's phase fluctuations. One of the criteria for analyzing tripartite entanglement (20) is written directly in terms of these correlations, as sums of variances V involving the three fields.

$$\begin{aligned} V_0 &= \Delta^2 \left(\frac{p_1 - p_2}{\sqrt{2}} \right) + \Delta^2 \left(\frac{q_1 + q_2}{\sqrt{2}} - \alpha_0 q_0 \right) \geq 2 \\ V_1 &= \Delta^2 \left(\frac{p_0 + p_1}{\sqrt{2}} \right) + \Delta^2 \left(\frac{q_0 - q_1}{\sqrt{2}} - \alpha_2 q_2 \right) \geq 2 \\ V_2 &= \Delta^2 \left(\frac{p_0 + p_2}{\sqrt{2}} \right) + \Delta^2 \left(\frac{q_0 - q_2}{\sqrt{2}} - \alpha_1 q_1 \right) \geq 2 \end{aligned} \quad (1)$$

It suffices to violate two of these inequalities to demonstrate tripartite entanglement. The p_i ($i = 0, 1, 2$) represent the amplitude quadratures of the fields, the q_i ($i = 0, 1, 2$) stand for their phase quadratures, and the α_i ($i = 0, 1, 2$) values are free parameters, chosen to maximally violate the inequalities. Phase and amplitude

¹Instituto de Física, Universidade de São Paulo, Post Office Box 66318, São Paulo, SP 05314-970, Brazil. ²Max Planck Institute for the Science of Light, Günther-Scharowsky-Strasse 1/Bau 24, 91058 Erlangen, Germany. ³University of Erlangen-Nuremberg, Staudtstrasse 7/B2, 91058 Erlangen, Germany.

*To whom correspondence should be addressed. E-mail: nussen@if.usp.br